Self-Assembled Complexes of Diazosulfonate Polymers with Low Surface Energies

Andreas F. Thünemann,*,† Ute Schnöller,‡ Oskar Nuyken,‡ and Brigitte Voit§

Max Planck Institute of Colloids and Interfaces, Am Mühlenberg, 14476 Golm, Germany; Technische Universität München, Lehrstuhl für Makromolekulare Stoffe; and Institut für Polymerforschung Dresden

Received June 2, 1999; Revised Manuscript Received August 25, 1999

ABSTRACT: The structures of the water-insoluble complexes of acrylate-based copolymers containing diazosulfonate groups and a fluorinated cationic surfactant (Hoe L-3658-1) were examined by X-ray diffraction, contact angle measurements, differential scanning calorimetry, and spectroscopic methods (IR, UV−vis, fluorescence). The structures of the complexes were shown to be lamellar and determined by using Ruland's interface distribution function procedure. Remarkably low critical surface tensions were found, indicating the formation of ordered layers of fluorocarbon segments at the surfaces of the complexes. Fine-tuning of the complex structures was achieved by varying the composition of the copolymers as well as the pH value present at the time of preparation. The formation of excimers was found to be strongly influenced by the complex structure.

Introduction

Polyelectrolyte−surfactant complexes in the solid state are considered to be promising for the development of smart materials that are characterized by self-organized supramolecular structures.[1] The simplicity of their synthesis and the variability of these mesomorphous materials are attractive features that simplify the "fine-tuning" of the resultant structures. We have reported on a number of polyelectrolyte−surfactant complexes that form low surface energies.[2−5] Products produced from similar complexes have been put on the market, for example, as dirt repellent and low-friction coatings.[6] It was shown earlier that polyelectrolytes containing diazosulfonate chromophores are useful for the preparation of solid complexes with nonfluorinated surfactants.[7] In this work we report on complexes of anionic polyelectrolytes that contain diazosulfonate groups and a commercially available fluorinated cationic surfactant (Hoe-L-3658-1).

Experimental Section

Materials. The diazosulfonate-containing acrylamido-4-phenyldiazosulfonate (monomer **M** (see Figure 1 for polymers) was prepared in analogy to the procedure described earlier[8] using acryloyl chloride instead of methacryloyl chloride. Acrylic acid (Fluka), hydroxypropyl acrylate (Fluka), methyl methacrylate (Fluka), and methyl acrylate (Fluka) were purified by passing through a basic aluminum oxide column to remove the stabilizer and were then distilled. *N*-Vinylcarbazole (Fluka), azobis(cyanovaleric acid) (Fluka), and dimethyl sulfoxide (Aldrich) were used without further purification. Hoe-L-3658-1 (Clariant) is a cationic fluorinated surfactant with a pendent perfluorinated alkyl chain $CF_3(CF_2)_n-(CH_2)_2-N^+(alkyl)_3I^-$ ($n \simeq 5$). Details about the chain length distributions were not given by the supplier. Hoe-L-3658-1 is commonly used as an active spreading agent.[9] 2,2,2-Trifluorethanol (Aldrich, 99,5%) was used as a solvent for the complexes.

Synthesis of Polyelectrolytes. All free radical polymerizations were carried out in a 10% aqueous solution at 70 °C for 17 h. Polymer **Pa** (used for the preparation of complex **a** and **c**) was synthesized from 5.5 mmol (1.4 g) of **M** and 7.8 mmol (0.56 g) of acrylic acid similar to the synthesis of diazosulfonate polymers described earlier.[8] The reaction was carried out in water with 0.68 mmol (0.19 g) of 4,4′-azobis-(cyanovalerianic acid) as initiator. **Pe** (used for the preparation of complex **e**) was prepared under the same conditions from 7.2 mmol (2.0 g) of **M**, 10.8 mmol (0.93 g) of methyl acrylate, and 0.95 mmol (0.26 g) of azobis(cyanovaleric acid). The polyelectrolytes were purified by dialysis in water. After evaporation of the water they were dried for 24 h in a vacuum at 50 °C. The yields were 1.9 g (92%, **Pa**) and 2.8 g (89%, **Pe**). Analysis of **Pa**: ^{1}H NMR (D_2O, δ in ppm) 1.1−3.0, 7−8. GPC: M_n = 7520 g/mol; M_w = 8800 g/mol; M_w/M_n = 1.17. Analysis of **Pe**: ^{1}H NMR (D_2O, δ in ppm) 0.9−4.1, 6.8−8.2. GPC: M_n = 7500 g/mol; M_w = 9510 g/mol; M_w/M_n= 1.28. **Pb** (used for the preparation of complex **b** and **d**) was synthesized using 5.0 mmol (1.4 g) of **M**, 7.6 mmol (0.55 g) of acrylic acid, 0.0500 g of *n*-vinylcarbazole, and 0.26 mmol (0.074 g) of azobis-

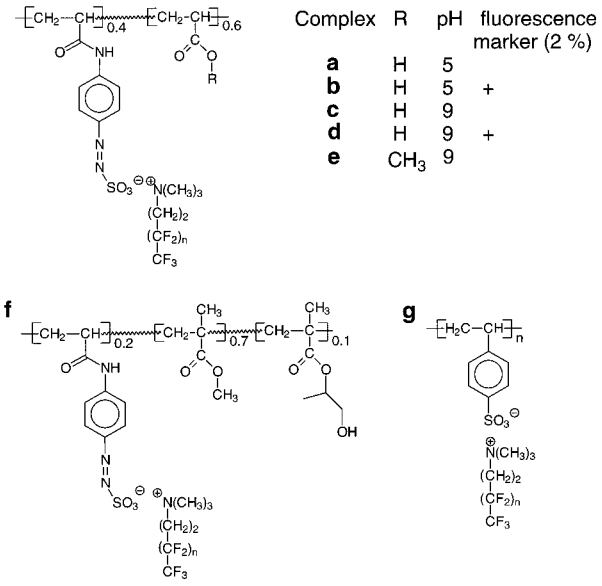

Figure 1. Complexes of poly[(acrylic acid)-*co*-(acrylamidophenyldiazosulfonate)] **(a−e)**, poly[(acrylamidophenyldiazosulfonate)-*co*-(1-hydroxy-2-methylethyl methacrylate)-*co*-(methacrylate)] **(f),** and poly(styrenesulfonate) **(g)**.

† Max Planck Institute of Colloids and Interfaces
‡ Technische Universität München
§ Institut für Polymerforschung Dresden
* Corresponding author.

10.1021/ma990868d CCC: $18.00
Published on Web 10/12/1999

(cyanovaleric acid). The polymerization was performed at the same conditions as for **Pa**, but dimethyl sulfoxide was used as solvent. For isolation of **Pb** the solution was diluted with 80 mL of methanol, precipitated in 2 L of ether, and dialyzed for 3 days. The yield was 1.3 g (65%). Analysis of **Pb**: ^{1}H NMR-(D_2O, δ in ppm) 1−4, 6.8−8.2. GPC: M_n = 7480 g/mol; M_w = 9450 g/mol; M_w/M_n = 1.26.

The preparation of **Pf** (used for the preparation of complex **f**) was similar to the procedure described earlier[8] with a reaction temperature of 70 °C. 1.0 g of **M**, 0.24 g of hydroxypropyl acrylate, and 1.2 g of methyl methacrylate were polymerized using 0.14 g of azobis(isobutyronitrile) in a dioxane/water (4/1) solution. The yield was 2.2 g (92%). Analysis of **Pf**: ^{1}H NMR (δ-DMSO, δ in ppm) 0.5−2.5, 3.5−4, 7.5−8, 9.2−9.7. GPC: M_n = 16 750 g/mol; M_w = 43 600 g/mol; M_w/M_n = 2.6. The thermal behavior of the polyelectrolytes **Pa**, **Pb**, **Pe**, and **Pf** was detected by DSC measurements. The decomposition of the azosulfonate functions started above 200 °C and had a maximum decomposition rate at 220−230 °C. In the UV/vis spectra of the copolymers an intensive absorption with a maximum at 331 nm was found which refers to the diazosulfonate group. The sodium salt of poly(styrenesulfonate) **Pg** was made by sulfonation of anionically polymerized polystyrene (M_w = 32 900 g/mol, M_w/M_n < 1.03) using H_2SO_4/P_2O_5 and the Vink procedure.[10] The degree of sulfonation was determined with elemental analysis and exceeded 0.90. **Pg** was dialyzed against pure water and freeze-dried.

Preparation of Complexes. A solution of 0.2 g of polyelectrolyte in 20 mL of water was stirred at room temperature, and 1.0 equiv of the fluorinated surfactant Hoe-L-3658-1 (dissolved in 20 mL of water) was added in droplets. (The stoichiometry was calculated with respect to the charges.) The solid polyelectrolyte−surfactant complexes precipitated after combining the two solutions and were obtained as white (complex **g**) or yellow to brown precipitates (complex **a** to **f**). The pH present at preparation was adjusted using 0.1 N HCl (see Figure 1). The complexes were isolated, washed three times with 100 mL of water, and dried for 24 h. Yields were between 0.3 and 0.5 g (54% **a**, 56% **b**, 72% **c**, 79% **d**, 54% **e**, 63% **f**, 43% **g**). The complexes were dissolved in 2,2,2-trifluoroethanol and cast into molds of aluminum coated with Teflon. After the evaporation of the solvent, films of the complex could be easily removed from the mold.

Measurements. The weight- and number-average molecular weigths (M_w and M_n, respectively) of the polyelectrolytes were determined by gel permeation chromatography (GPC, 0.5 mol/dm^3 ammonium formiate, OH-Pak 804 HQ column by Shodec, refraction index detector). A mixture of water and acetonitrile (20/80) was used as eluent and polyethylene gylcol as molecular weight standard. Wide-angle X-ray scattering (WAXS) measurements were carried out with a Nonius PDS120 powder diffractometer using transmission geometry. A FR590 generator was used as the source of Cu Kα radiation, monochromatization of the primary beam was achieved by means of a curved Ge crystal, and the scattered radiation was measured with a Nonius CPS120 position-sensitive detector. The resolution of this detector is about 0.018°. We performed the small-angle X-ray scattering experiments with a Kratky compact camera (Anton Paar, Austria), equipped with a stepping motor and a counting tube with an impulse-height discriminator. The light source was a conventional X-ray tube with a fixed copper target operating at 40 mA and 30 kV.

Contact angle measurements were performed on a Krüss G10 contact angle goniometer; the angles reported here are the average of five measurements. The advancing contact angle was determined by injecting a 5 μL liquid droplet, the receding contact angle was measured by removing about 3 μL of liquid from the droplet, and the static contact angle was obtained from a droplet (ca. 5 μL) on the surface. Linear alkanes, methyl-terminated poly(dimethylsiloxane) oligomer (Geltest Inc.), diiodomethane, and water (Millipore) were used as test liquids.

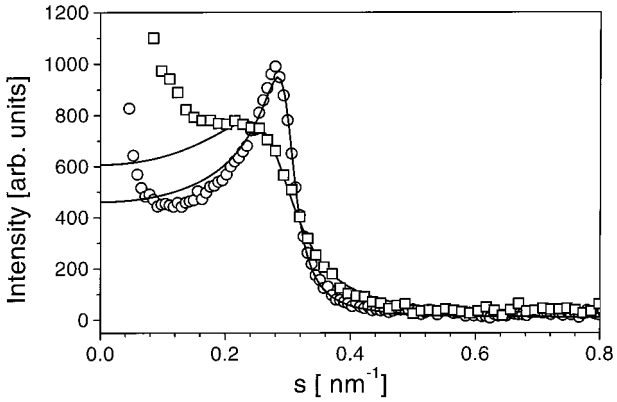

Figure 2. Small-angle X-ray scattering curve of complex **a** (circles) and **f** (squares) and fits according to eq 1.

Results and Discussion

It is well-known that mixing equimolar amounts of water solutions of polyelectrolyte chain units and surfactants results in water-insoluble complexes of stoichiometric complexes.[11,12] In our experiments, mixing equimolar amounts of polyelectrolyte (see Figure 1, structures **a** to **g**) and fluorinated surfactant resulted in complexes that precipitate immediately. After purification by washing with water, the complexes were dried in a vacuum, subsequently soluted in trifluorethanol, and cast into transparent films. The nature of surfactant chain packing in the complexes was determined by wide-angle X-ray scattering (WAXS). In the WAXS patterns of all complexes, only a broad reflection was found, which corresponded to a Bragg spacing of 0.52 nm. This can be attributed to an amorphous packing of fluorinated alkyl chains. This finding is similar to that observed for complexes of cationic copolymers of low charge density with perfluorodecanoic acid, but this is in contrast to a complex of poly(diallyldimethylammonium) chloride homopolymer with perfluorodecanoic acid, which was found to be partially crystalline.[3] The absence of crystallinity for the complexes **a** to **g** can probably be attributed to the relatively short length of the fluorinated chain (C_6F_{13}), which is too short to allow a side-chain analogues crystallinity.

Supramolecular Structures. Small-angle X-ray scattering experiments were carried out in order to study the mesomorphous character of these complexes. The curves for powder and film samples were identical within the range of experimental errors. Typical scattering curves, as found for complexes **a** and **f**, are shown in Figure 2. An intense maximum that confirms the assumption of a microphase-separated system was found in the scattering curves of all complexes. Weak reflections of a second order were observed in the curves of complexes **d** and **g**, which is indicative of a lamellar structure. A detailed evaluation of the data has to be carried out for a precise assignment of the phase structure. First, to determine the repeat units, the smearing effect of the camera system has to be taken into account. The use of a Kratky camera causes a characteristic peak profile due to the slit-length smearing of the experimental equipment. The broader the peak, the more the peak maximum deviates from the real reflex position s_h, which would, for example, be measured with a pinhole system. To determine the reflex position and its integral width, b, the analytical expression of a slit-smeared, three-dimensional Lorentzian distribution, was used:[13]

$$J(s) = \frac{1}{2s_h}\left(\frac{(A^2 + B^2)^{1/2} - A}{2(A^2 + B^2)}\right) \quad (1)$$

where $A = b^2 + \pi^2(s^2 - s_h^2)$ and $B = 2\pi b s_h$. J represents the slit-smeared intensity obtained by using a Kratky camera, and s_h is the reflex position without slit-smearing effects. This expression was fitted to the Kratky peaks, resulting in s_h and b values of 0.280 $nm^{-1} < s < 0.333$ and 0.071 $nm^{-1} < b < 0.190$ (see Table 1). It can be assumed from the similarity of the values that the complexes are isomorphic with smectic A-like complexes of poly(acrylic acid) and poly(methacrylic acid) with Hoe-L-3658-1 described earlier.[14] Additional information concerning these structures can be obtained from the asymptotic decrease of the scattering curve. At larger angles, the scattered intensity decreases with the third power of the scattering vector. This is in accordance with Porod's law.[15,16] Such a scaling law is a strong indication of a two-phase system with sharp interface boundaries. Porod's law is given by[15]

$$\lim_{s\to\infty} 4\pi^2 s^3 J(s) = \frac{k}{l_p} \quad (2)$$

where the scattering vector is defined as $s = 2/\lambda \sin\theta$, and θ is the Bragg angle, λ is the wavelength, J is the slit-smeared scattering intensity, and l_p is the average cord length. k is the invariant, which is given by the expression

$$k = 2\pi \int_0^\infty sJ(s)\, ds \quad (3)$$

The main source of error in the range of validity covered by Porod's law is the scattering due to density fluctuations and the widths of the domain boundary.[17] The linear behavior of the scattering curve in a $s^3J(s)-s^3$ plot (Figure 3) proves that the only deviation from Porod's law is a three-dimensional homogeneous density fluctuation, which is given by the slope of the straight line. A broader transition or a statistical structuring of the domain boundary, as typically observed in microphase-separated block copolymers,[18] can be excluded. Small deviations from a sharp boundary would indicate a significant deviation from Porod's law.[17] Therefore, we can conclude that the phase boundaries of the complexes are of the order of 1−2 atomic distances. Using eq 2, the average chord lengths were calculated to be in the range from 1.19 to 1.30 nm, which is similar to the polymeric complexes of siloxane surfactants we investigated earlier.[19] The simplest complex structure that is in agreement with these numbers is a microphase-separated model constructed from a smaller ionic phase (polyelectrolyte plus ionic headgroups) and a larger nonionic phase (hydrophobic moieties). The repeat unit of a lamellar system d is given by $d = d_1 + d_2$, where d_1 and d_2 are the thicknesses of the two lamellae. Their values can be determined by calculating the interface distribution function $g(r)$,[20] which is defined as the second derivative of a one-dimensional autocorrelation function for positive values of the distance r in real space. The interface distribution function can be computed by a combination of the inverse Fourier transformation and slit desmearing given by the expression

$$g(r) \propto \int_0^\infty G(s)\left(4J_0(2\pi rs) - \frac{1 + 4\pi^2 r^2 s^2}{\pi rs} J_1(2\pi rs)\right) ds \quad (4)$$

Table 1. Structure Parameters Determined by Small-Angle X-ray Analysis

complex	d [nm]	d_1 [nm]	d_2 [nm]	l_p nm	S/S_0	s [nm^{-1}]	b [nm^{-1}]
a	3.35	1.15	2.20	1.20	1.26	0.299	0.071
b	3.41	1.11	2.30	1.19	1.24	0.293	0.120
c	3.15	1.10	2.05	1.30	1.10	0.317	0.108
d	3.17	1.07	2.10	1.20	1.18	0.315	0.083
e	3.18	1.10	2.08	1.28	1.12	0.314	0.122
f	3.56	*a*	*a*	*a*	*a*	0.280	0.190
g	2.93	1.00	1.93	1.19	1.11	0.333	0.094

[a] Values cannot be determined due to absence of an asymptotic scaling according to Porod's law.

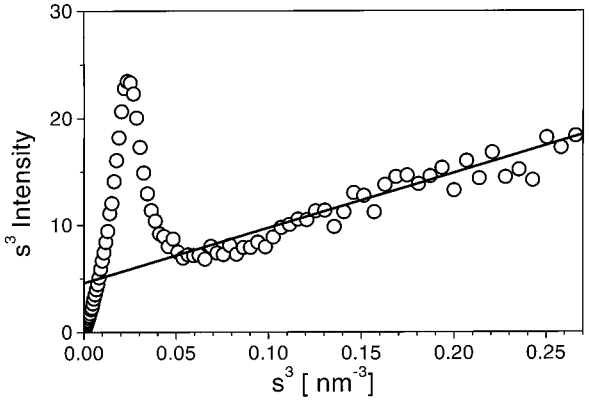

Figure 3. s^3J-s^3 plots of the small-angle X-ray scattering of complex **a** (circles) and their ideal behavior according to Porod's law (solid line).

where J_n is the Bessel function of the first kind and the nth order, and $G(s)$ is the interference function defined by

$$G(s) \propto [\lim_{s\to 0} s^3\, J(s)] - s^3 J(s) \quad (5)$$

The interface distribution function can be written in the form[20]

$$g(r) \propto h_1 + h_2 - 2h_{12} + h_{121} + h_{212} - 2h_{1212} + \ldots \quad (6)$$

where h_i represents the normalized distributions of the distances between interfaces, measured at a perpendicular to the planes of the lamellae. A model that can describe the statistics of lamellar phases is the lattice model, in which the statistics are described by the distributions $h_1(d_1)$ and $h_2(d)$ of the lamellar thicknesses.[18,21] In Figure 4, for example, the interface distribution function computed from the scattering curve of complex **a** and the best fit using the lattice model have been plotted. As shown in Table 1, the thicknesses of the ionic layers of complex **a** to **e** is in a narrow range between 1.07 and 1.15 nm, and the thickness of the hydrophobic layers varies between 2.08 and 2.30 nm. The thickness of an ionic layer of complex **g** (1.00 nm) is slightly lower, which is in agreement with its lower ratio of mass per charge. In contrast to complexes **a** to **e** and **g**, no asymptotic behavior according to Porod's law was found for complex **f**. Consequently, the thicknesses d_1 and d_2 cannot be computed. It must be assumed that the phase separation of **f** is not as strong as found for the other complexes. A

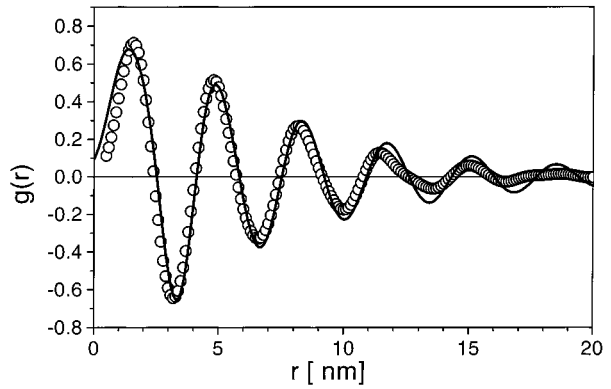

Figure 4. Interface distribution function computed from the experimental values for complex **a** (circles). The solid line is the theoretical curve with lamellar thicknesses of $d_1 = 1.15$ nm and $d_2 = 2.20$ nm.

possible reason for this is the lower amount of ionic monomers of **f** (20 mol %). For the other complexes the amount of ionic monomers (in mole percent) is 100 (**c**), 98 (**d**), 40 (**a** and **e**), and 38 **(b)**, which is high enough for a strong phase separation. In addition to the lamellar thicknesses, the curvature of the interface between ionic and nonionic domains is an important characteristic of the description of the complex morphology. If the interfaces of the lamellae are completely planar, and the lateral dimensions are large compared to the thicknesses of the lamellae, the total interface area per volume is given by $S_0/V = 2/d$. But, if the interface is not planar, the total interface area S obtained from l_p is larger than S_0 obtained from L. A measure of the planarity of the interfaces is obtained from the ratio

$$\frac{S}{S_0} = \frac{2d_1d_2}{Ll_p} \tag{7}$$

Using eq 7, the surface ratios were found to be in the range 1.10−1.26 (see Table 1). The surface ratios of **c** (1.10), **e** (1.12), and **g** (1.11) are small and nearly identical and can be seen as essentially flat interface boundaries. The slightly higher value of **d** (1.18) compared to that of **c** (1.10) may be due to the presence of the fluorescence label, which enhances the waviness to a small extent. The larger values of **a** (1.26) and **b** (1.24) are indicative of a significantly higher waviness of the interfaces. These values are similar to those determined by Ruland et al.[18] for the lamellar structures of diblock copolymers, and for polyelectrolyte−surfactant complexes in the solid state such undulations are typically due to packing constrains.[22,23]

Surface Energies. Films of complexes **a** to **g** were prepared by casting 0.1−0.5% (w/w) complex solutions on glass surfaces. The complex solutions were dried at room temperature in dry air, resulting in thin transparent coatings with thicknesses of about 500 nm. Dynamic contact angles θ of the test liquids with different surface tensions were measured by means of the sessile drop method.[24] The results are summarized in Table 2. It was found in particular that all nonpolar liquids, which spread readily on uncoated surfaces, showed high contact angles on complex-coated surfaces. However, direct measurement of the surface energies of nonelastomeric solid materials is not simple. For practical reasons, procedures based on contact angle measurements are normally used.[25−31] Neumann and Li derived an equation, by which it is possible to calculate the surface free energy of a solid,[32] such that

$$\cos\theta = -1 + 2\sqrt{\frac{\gamma_s}{\gamma_l}}\exp(-\beta(\gamma_l - \gamma_v)) \tag{8}$$

where β is a constant (0.000 124 7 $m^2\ mJ^{-1}$). Thus, the surface energy γ_s can be determined from experimental contact angles and the liquid surface tension γ_l. The surface energies calculated using eq 8 range from 11.4 to 16.9 mN/m for all test liquids with surface tensions in the range 18.4−50.0 mN/m (Table 2). These values are of the same order of magnitude as the surface energies found in fluorinated polymer (FC-725)-coated silicon wafers.[31] These range from 11.8 to 13.2 mN/m. The critical surface tension γ_c of a surface can often be determined by the contact angles of a homologous series of nonpolar liquids.[25] γ_c defines the wettability of a solid by fixing the lowest surface tension a liquid can have and still exhibit a contact angle greater than 0°. The γ_c value of a surface is usually obtained from a Zisman plot of the contact angles;[25] such a plot of cos θ against the surface tensions of liquids γ_l is a straight line with the slope m:

$$\cos\theta = 1 + m(\gamma_l - \gamma_c) \tag{9}$$

The extrapolation of γ_l to cos $\theta = 1$ gives γ_c. Zisman plots (see Figure 5 and Table 3) result in critical surface tensions of 7.5 mN/m (complex **c**) to 13.2 mN/m (complex **f**). These values are significantly lower than that expected for a surface enriched predominantly with CF_2 groups (ca. 18.5 mN/m) and are higher than that expected for an oriented close-packed monolayer of perfluorododecanoic acid (6 mN/m).[33] As recently demonstrated by Ober et al.,[34] such surface energies are typically found in fluorinated side-group block copolymers in the smectic A phase. Therefore, in combination with the X-ray results, the complexes are similar to a smectic A side-chain polymer. In contrast to this, the fluorinated chains in our samples are not bound covalently but ionically. Considering the critical surface energy data, it seems that the complex surfaces were strongly enriched with lose-packed $-CF_3$ groups. The packing increases along line **f**, **a**, **c**. This results in a parallel shift of the straight lines (Figure 5). It must be stressed here that although γ_c values are widely used for surface characterization, there is no theoretical justification for equating the critical surface tension with the surface energy of a material. The wettability data were also used to determine the dispersion force component of the surface energy γ_s^d by using the Girifalco−Good−Fowkes−Young equation,[26,27] which has the form

$$\cos\theta = -1 + 2\sqrt{\frac{\gamma_s^d}{\gamma_l}} \tag{10}$$

and has been theoretically justified. This equation is fitted to the plot of cos θ against $(1/\gamma_l)^{1/2}$ for dispersive liquids with the ordinate of the best linear fit located at −1, the gradient being $2(\gamma_s^d)^{1/2}$. The Girifalco−Good−Fowkes−Young plots are used to show the dynamic advancing contact angle data (Figure 6). Linear fits result in dispersive surface energies of $\gamma_s^d = 11.4 \pm 0.2$ mN/m (complex **c**) and 16.2 ± 0.3 mN/m (complex **f**). All results are given in Table 3 where it can be seen

Table 2. List of Contact Angles of Different Solvents on Glass Surfaces Coated with Complex Solutions at 20 °C[a]

solvent	surf tension (mN/m)	advancing angle (deg)[b]	stationary angle (deg)[b]	receding angle (deg)[b]	γ [mN/m]
		Complex **a**			
hexane	18.4	41	40	31	14.2
PDMS[c]	18.7	41	40	32	14.5
octane	21.8	51	49	44	14.7
decane	23.9	56	55	46	14.8
dodecane	25.4	61	60	51	14.4
hexadecane	27.6	64	62	51	14.9
methylene iodide	50.0	95	91	73	14.3
water	72.7	87	86	54	31.1
		Complex **c**			
hexane	18.4	53	50	41	11.9
PDMS[c]	18.7	54	54	47	11.9
octane	21.8	62	61	50	12.0
decane	23.9	66	65	48	12.2
dodecane	25.4	72	70	61	11.4
hexadecane	27.6	74	73	60	11.9
methylene iodide	50.0	100	95	75	12.2
water	72.7	96	95	70	25.5
		Complex **e**			
hexane	18.4	48	48	41	12.9
PDMS[c]	18.7	49	48	42	12.9
octane	21.8	57	55	52	13.2
decane	23.9	63	61	55	13.0
dodecane	25.4	66	65	58	13.1
hexadecane	27.6	70	68	58	13.1
methylene iodide	50.0	99	98	74	12.6
water	72.7	90	85	30	29.2
		Complex **f**			
hexane	18.4	33	30	26	15.6
PDMS[c]	18.7	34	34	31	15.7
octane	21.8	45	44	40	16.0
decane	23.9	49	49	40	16.6
dodecane	25.4	53	51	43	16.6
hexadecane	27.6	57	55	39	16.9
methylene iodide	50.0	92	90	78	15.6
water	72.7	55	52	44	50.8
		Complex **g**			
hexane	18.4	49	45	42	12.7
PDMS[c]	18.7	50	49	45	12.7
octane	21.8	58	57	53	13.0
decane	23.9	63	63	55	13.0
dodecane	25.4	68	68	59	12.5
hexadecane	27.6	70	67	57	13.0
methylene iodide	50.0	97	94	76	13.4
water	72.7	108	104	73	18.2

[a] The surface tensions of the test liquids and the advancing, stationary, and receding contact angles measured by a Krüss contact angle goniometer are listed. The surface tensions of the complex surfaces γ were calculated using the equation of Neumann and Li (eq 8). [b] Error of measurement ca. 1°. [c] Commercial product of poly(dimethylsiloxane) oligomers (trimethylsiloxy terminated) from Geltest Inc.

that the highest surface energy of 16.2 mN/m was determined for the complex **f**, which contains an amount of only 20 mol % of charged monomers in the polymeric backbone. Furthermore, the OH groups present in the polymer may be responsible for the higher surface energy. From the very similar values found for complexes **a** and **b** (14.0 and 14.2 mN/m) as well as for **c** and **d** (11.4 mN/m both), we can conclude that the fluorescence markers (2 mol %) do not affect the surface energy. A significant effect on the surface energy was found, whether the complexation was performed with an acidic or a basic pH value. Complexes **a** and **b** were prepared at a pH value of 5, at which the acidic moieties are protonated; the polymeric backbone contains 40 mol % ionic monomers. Under these conditions only the sulfonate groups were complexed by the cationic surfactant, and the 60 mol % carboxylic acid groups remained, which may enhance the surface energy. Applying a pH of 9, the carboxylic moieties are deprotonated and were able to complex with cations. Under this condition 100 and 98 mol % in the case of complexes **c** and **d**, respectively, could be complexed. The surface energy in these cases (11.4 mN/m) was significantly lower than that determined for **a** and **b** (14.0 mN/m). For the complex of another polymer with 100 mol % ionic monomers (styrenesulfonate) **g**, the surface energy of 12.3 mN/m was close to the low values of **a** and **b**. Here it is obvious that the denser the packing of the fluorinated surfactant along the polymeric backbone, the lower the surface energy. Complex **e**, which has 40 mol % ionic monomers, has a significantly lower surface energy than **a** or **b**. This can be explained by the less polar methacrylate group compared to the carboxylate group. These values are slightly higher than those found for a highly fluorinated side-chain homopolymer *p*-[(perfluorooctylethylene)oxy]methyl]styrene (9.3 mN/m[29]) and some other fluorinated polyelectrolyte−surfactant complexes.[2] However, the γ_c and γ_s^d values indicate a high enrichment of CF_3 groups on the complex surface. It is particularly interesting that the contact

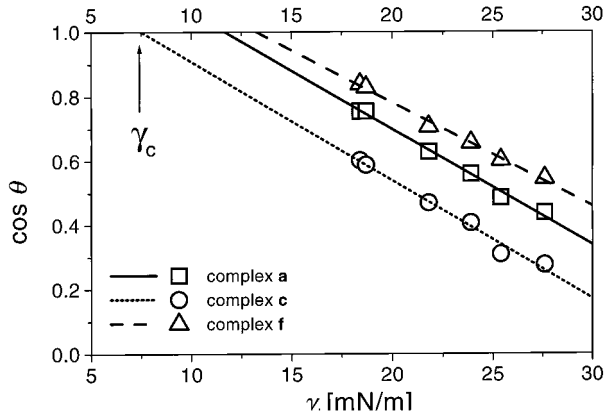

Figure 5. Zisman plots for complex coated glass surfaces. Points are obtained with (1) hexane, γ_l = 18.4 mN/m; (2) PDMS, γ_l = 18.7 mN/m; (3) octane, γ_l = 21.8 mN/m; (4) decane, γ_l = 23.9 mN/m; (5) dodecane, γ_l = 25.4 mN/m; and (6) hexadecane, γ_l = 27.6 mN/m. The critical surface tension of complex **a** was calculated to be 11.7 mN/m by extrapolating a linear fit (solid line) of the cos θ (squares) to cos θ =1. For complex **c** (circles) a critical surface tension of 7.5 mN/m was determined (dashed line), and for complex **f** (triangles) γ_c is 13.2 mN/m. Advancing contact angles were used for cos θ.

Table 3. Zisman Critical Surface Energies γ_c and the Dispersive Surface Energies γ_s^d According to the Girifalco−Fowkes−Young Equation of Complex Films on Glass

complex	γ_c [mN/m]	γ_s^d [mN/m]
a	11.7 ± 1.5	14.0 ± 0.3
b	11.9 ± 1.2	14.2 ± 0.4
c	7.5 ± 1.9	11.4 ± 0.3
d	9.1 ± 1.4	11.4 ± 0.2
e	9.2 ± 0.9	12.4 ± 0.3
f	13.2 ± 1.4	16.2 ± 0.3
g	8.7 ± 1.8	12.3 ± 0.3

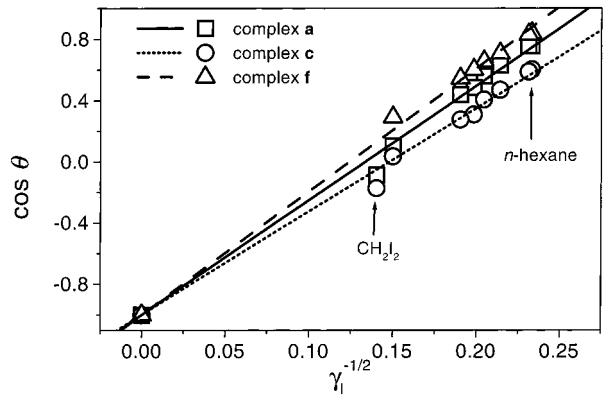

Figure 6. Girifalco−Good−Fowkes−Young plots for the determination of the dispersive surface energy of complex coated glass surfaces. From left to right the points are values obtained with (1) methylene iodide, γ_l = 50.0 mN/m; (2) α-bromonaphthalene, γ_l = 44.0 mN/m; (3) hexadecane, γ_l = 27.6 mN/m; (4) dodecane, γ_l = 25.4 mN/m; (5) decane, γ_l = 23.9 mN/m; (6) octane, γ_l = 21.8 mN/m; (7) PDMS γ_l = 18.7 mN/m; and (8) hexane γ_l = 18.4 mN/m. γ_s^d were calculated from the slope to be 14.0 mN/m for complex **a** (squares represent measured angles, the solid line the least-squares fit), 11.4 mN/m for complex **c** (circles, dotted line), and 16.2 mN/m for complex **f** (triangles, dotted line).

angles of water (the most polar test liquid with γ_l = 72.7 mN/m) is only as high as or smaller than that of methylene iodide (γ_l = 50.0 mN/m). The surface energies calculated using eq 8 increase in the order of complex **g** (18.2 mN/m), **c** (25.5 mN/m), **e** (29.2 mN/m), **a** (31.1 mN/m), and **f** (50.8 mN/m). The low surface energies determined for nonpolar liquids were reproduced, even when the complex coated surfaces were dried after exposure to water. This indicates a reversible surface reconstruction of the complex surface after it has been in contact with water. Surface reconstruction phenomena are widespread in polymer coatings, such as self-organizing semifluorinated side-chain ionenes[30] and even polymers containing only a few polar groups, such as Teflon-PFA.[35] It is worth noting that the surface reconstruction of the complex when in contact with water seems to be very fast, as shown by the static constant contact angle of water which adjusts to an equilibrium within a few seconds. The degree and velocity of surface reconstruction are assumed to be dependent on several factors, such as the number of polar groups within a distance of about 1 nm from the surface and the flexibility of the polymeric backbone, which is affected by the glass transition temperature.

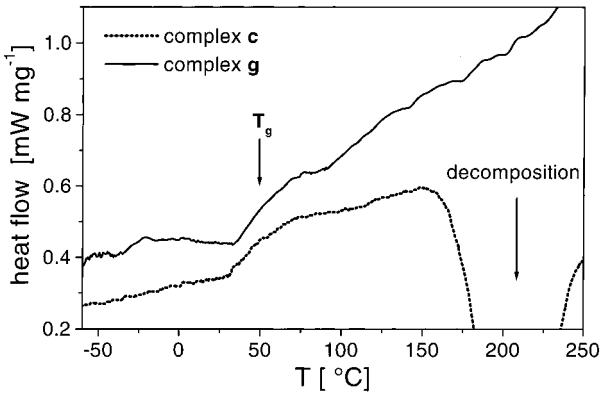

Figure 7. DSC thermograms of the complexes **c** and **g** during heating.

Thermal Analysis. The thermal behavior of the complexes was investigated by DSC. Typical DSC thermograms are shown in Figure 7. Weak glass transitions could be detected at several degrees above room temperature for the complexes **c** (34 °C), **d** (27 °C), **e** (31 °C), and **f** (30 °C). Above a temperature of 170 °C decomposition sets in, which reaches a maximum at about 200−220 °C. For complexes **a** and **b** we were not able to detect glass transitions, but their decomposition behavior is essentially identical to that of the other azo group containing complexes. The absence of glass transitions is typical for polyelectrolytes, and therefore it seems not to be very surprising that in the cases of complexes **a** and **b** no glass transitions could be detected. The highest glass transition, at about 48 °C, was detected for **g**, a complex that contains no azo groups. Such a high value may be explained by a higher rigidity of the polystyrenesulfonate backbone compared to that of the polymeric backbones of the other complexes. It can be seen in Figure 7 that below 250 °C no significant decomposition was found. Therefore, the decomposition process was regarded as the thermal decomposition of the azo groups. This assumption was supported by investigations of the thermal decomposition of azosulfonate-containing polymers and azosulfonate-containing surfactants.[36] No other thermal transitions were observed in the temperature range from −100 to 170 °C. We conclude that the thermal stability of the complexes is determined mainly by the stability of the polymer.

Spectroscopic Properties. Infrared Spectroscopy. The significant difference observed in supramo-

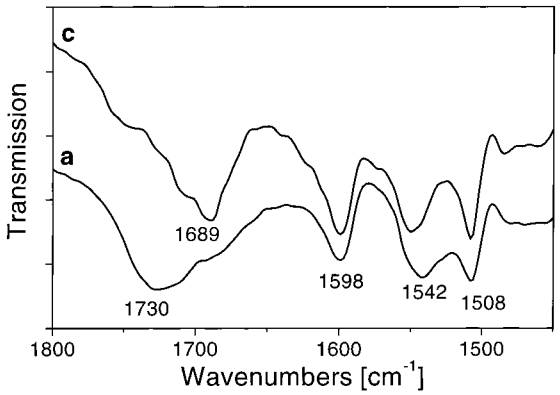

Figure 8. FTIR spectra of complexes **a** and **c**.

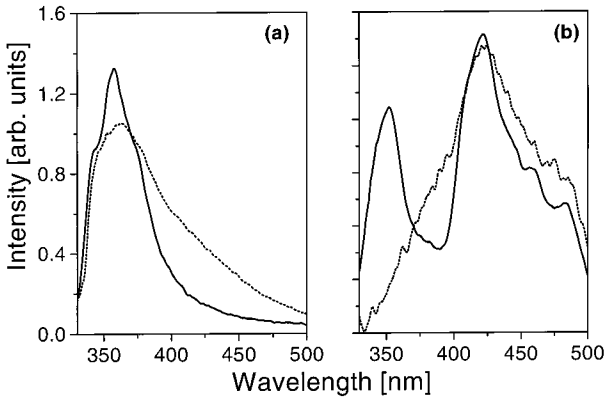

Figure 9. Steady-state fluorescence spectra. Typical emission spectra of complex **b** (dotted lines) and **d** (solid lines). The measurements were performed on solution (figure left) and on free-standing films (figure right). The excitation wavelength is 293 nm.

lecular structure, surface energies, and thermal properties between complexes **a**, **b** and **c**, **d** was suggested to result from different degrees of ionization of the carboxylic groups. This was then proved by IR measurements. In Figure 8 it can be seen that the carbonyl stretch vibration band of complex **a** is located at 1730 cm^{-1}, whereas that of complex **c** is located at 1689 cm^{-1}. These values can be assigned to the protonated and deprotonated form of the carboxylic acid moieties. Therefore, within the solid complex **a** about 40 mol % of the monomer units (SO_3^-) are charged and about 100 mol % in complex **c**. The aromatic ring vibrations can be found at 1598 and 1508 cm^{-1}; the band at 1542 cm^{-1} can be assorted to the amidic group.

The UV/vis spectra for all diazosulfonate-containing complexes show an absorption with maximum at 331 nm referring to the diazo group. Loss of the absorption was found after irradiation with UV light.

Fluorescence Properties. The difference between complexes **a, b** and **c, d** in their supramolecular order as well as in their surface properties may partly result from a different organization of the polyelectrolyte chains within the complexes. To investigate the polymer chain organization in **b** and **d**, acrylic acid and **M** were copolymerized (**Pb**) with 2 mol % *N*-vinylcarbazole, which acts as fluorescence label. At an excitation wavelength of 293 nm, the free monomer shows a structured emission band at 350 nm, whereas for vinylcarbazole homo- and copolymers an additional emission band at lower energies is present due to the formation of excimers. The fluorescence of the polymers is dominated by the emissions of two excimer species: emission centered at ca. 420 nm originates from a conventional "sandwich-like" excited-state dimer, whereas the peaking at 370 nm was attributed to luminescence from a partially overlapped, "second" excimer.[37,38] It can be seen in Figure 9a that the emission spectra of diluted complex **b** and **d** solutions (5×10^{-3} % w/w) differ significantly. All spectra of Figure 9 have been normalized to equal intensity at 370 nm. The fluorescence intensity at 420 nm was found to be much higher for complex **b** (dotted line) than for complex **d** (solid line). Further, the monomeric emission at about 350 nm is higher for **d** than for **b**. From this, it can be concluded that in diluted solution the formation of conventional excimers is favored for complex **b**, whereas for complex **d** the uncorrelated, i.e., monomeric, emission is predominant. Therefore, at a high degree of complexation (complex **d**, 98 mol %) the tendency of excimer formation is lower than at a lower degree of complexation (complex **b**, 40%). This behavior was found to be even more pronounced for free-standing complex films (Figure 9b). In the spectrum of complex **b** (dotted line) most of the intensity is due to the "sandwich-like" excimer, and the monomer emission is negligible. The spectrum of complex **d** (solid line) is even dominated by the emission of this excimer, but the monomeric emission is still present to a considerable degree.

Conclusion

We have shown that the solid-state structures of the water-insoluble complexes formed by azosulfonate-containing polyelectrolytes and a fluorinated cationic surfactant are lamellar structures capable of forming low surface energies. A fine-tuning of the structures and the surface energies was achieved by varying the composition of the polymer backbone, the charge density, and the pH value.

Acknowledgment. We thank R. Kublickas for help in preparation of complexes, S. Förster for synthesis of polystyrenesulfonate, D. Ruppelt for performing the fluorescence spectroscopy, and the Max-Planck Society for their financial support.

References and Notes

(1) Ober, C.; Wegner, G. *Macromolecules* **1997**, *9*, 117.
(2) Thünemann, A. F.; Lieske, A.; Paulke, B. R. *Adv. Mater.* **1999**, *11*, 321.
(3) Thünemann, A. F.; Lochhaas, K. H. *Langmuir* **1998**, *14*, 4898.
(4) Thünemann, A. F.; Lochhaas, K. H. *Langmuir* **1999**, *15*, 4867.
(5) Thünemann, A. F.; Lochhaas, K. H. *Langmuir* **1999**, *15*, 6724.
(6) Products are on the market that form easy-to-clean surfaces. An example is the protection of walls from graffiti. Products with low friction are used for skiing and biathlon sports. Information supplied by Colloid Surface Technologies GmbH, Wiesbaden, Germany.
(7) Antonietti, A.; Kublickas, R.; Nuyken, O.; Voit, B. *Macromol. Rapid Commun.* **1997**, *18*, 287.
(8) Matusche, P.; Nuyken, O.; Voit, B.; Van Damme, M.; Vermeersch, J.; De Winter, W.; Alaerts, L. *React. Polym.* **1995**, *24*, 271.
(9) Information supplied by the manufacturer, Hoechst AG, Frankfurt, Germany.
(10) Vink, H. *Makromol. Chem.* **1981**, *182*, 279.
(11) Ponomarenko, E. A.; Tirrell, D. A.; MacKnight, W. J. *Macromolecules* **1998**, *31*, 1584.
(12) Goddard, E. D.; Ananthapadmanabhan, K. P. *Interactions of Surfactants with Polymers and Proteins;* CRC Press: Boca Raton, FL, 1993.
(13) Ruland, W., private communication.
(14) Antonietti, M.; Henke, S.; Thünemann, A. F. *Adv. Mater.* **1996**, *8*, 41.

(15) Porod, G. *Kolloid-Z.* **1951**, *124*, 83.
(16) Porod, G. *Kolloid-Z.* **1952**, *125*, 51.
(17) Siemann, U.; Ruland, W. *Colloid Polym. Sci.* **1982**, *260*, 999.
(18) Wolff, T.; Burger, C.; Ruland, W. *Macromolecules* **1994**, *27*, 3301.
(19) Thünemann, A. F.; Lochhaas, K. H. *Langmuir* **1998**, *14*, 6220.
(20) Ruland, W. *Colloid Polym. Sci.* **1977**, *255*, 417.
(21) Tswankin, D. Y.; Zubov, A. Y.; Kitaigorodskii, A. I. *J. Polym. Sci.* **1968**, *C16*, 4081.
(22) Antonietti, M.; Conrad, J.; Thünemann, A. F. *Macromolecules* **1994**, *27*, 6007.
(23) Micha, M. A.; Burger, C.; Antonietti, M. *Macromolecules* **1998**, *31*, 5930.
(24) Augsburg, A.; Grundke, K.; Pöschel, K.; Jacobasch, H.-J.; Neumann, A. W. *Acta Polym.* **1998**, 49, 417.
(25) Zisman, W. A. *Ind. Eng. Chem.* **1963**, *55*, 18.
(26) Fowkes, F. M. *J. Phys. Chem.* **1962**, *66*, 382.
(27) Girifalco, L. A.; Good, R. J. *J. Phys. Chem.* **1957**, *61*, 904.
(28) Drummond, C. J.; Georgaklis, G.; Chan, D. Y. C. *Langmuir* **1996**, *11*, 2617.
(29) Höpken, J.; Möller, M. *Macromolecules* **1992**, *25*, 1461.
(30) Wang, J.; Ober, C. K. *Macromolecules* **1997**, *30*, 7560.
(31) Kwok, D. Y.; Lam, C. N. C.; Li, A.; Leung, A.; Wu, R.; Mok, E.; Neumann, A. W. *Colloids Surf.* **1998**, *142*, 219.
(32) Li, D.; Neumann, A. W. *J. Colloid Interface Sci.* **1992**, *148*, 190.
(33) Hare, E. F.; Shafring, E. G.; Zisman, W. A. *J. Colloid Sci.* **1954**, *58*, 236.
(34) Wang, J.; Mao, G.; Ober, C. K.; Kramer, E. J. *Macromolecules* **1997**, *30*, 1906.
(35) Yasuda, H.; Okuno, T.; Sawa, Y.; Yasuda, T. *Langmuir* **1995**, *11*, 3255.
(36) Stasko, A.; Erentova, K.; Rapta, P.; Nuyken, O.; Voit, B. *Magn. Reson. Chem.* **1998**, *36*, 13.
(37) Johnson, E. G. *J. Chem. Phys.* **1975**, *62*, 4697.
(38) Grazulevicius, J. V.; Soutar, I.; Swanson, L. *Macromolecules* **1998**, *31*, 4820.

MA990868D